AIAA 2002-1116
Soot Surface Growth and Oxidation in Laminar Unsaturated-Hydrocarbon/Air Diffusion Flames

A.M. El-Leathy, F. Xu and G.M. Faeth
The University of Michigan,
Ann Arbor, Michigan 48109-2140

40th AIAA Aerospace Sciences Meeting & Exhibit
14-17 January 2002 / Reno, NV

AIAA 2002-1116

SOOT SURFACE GROWTH AND OXIDATION IN LAMINAR UNSATURATED-HYDROCARBON/AIR DIFFUSION FLAMES

A.M. El-Leathy*, F. Xu† and G.M. Faeth**
The University of Michigan, Ann Arbor, Michigan 48109-2140

ABSTRACT

The structure and soot surface growth and oxidation properties of round laminar coflowing jet diffusion flames were studied experimentally. Test conditions involved ethylene-, propylene-, propane- and benzene-acetylene-fueled diffusion flames burning in coflowing air at atmospheric pressure with the reactants at normal temperature. Measurements were limited to the axes of the flames and included soot concentrations, soot temperatures, soot structure, major gas species concentrations, radical (H, OH, O) species concentrations, and gas velocities. The results show that fuel decomposition yields significant acetylene concentrations at fuel-rich conditions, that soot formation begins where significant concentrations of both acetylene and H-radical are present, and that soot formation ends when acetylene concen-trations become small even in the presence of significant concentrations of H-radical. Present measurements of soot surface growth rates in diffusion flames were consistent with earlier measurements in both acetylene-fueled diffusion flames and in ethylene- and methane-fueled premixed flames, with results over this entire data base exhibiting encouraging agreement with existing Hydrogen-Abstraction/Carbon-Addition (HACA) soot surface growth mechanisms. It also was found that present surface oxidation rates in diffusion flames could be described reasonably well by the OH mechanism with a collision efficiency of 0.10, with no significant effect of fuel type, in good agreement with the classical premixed flame measurements of Neoh et al. (1980). Finally, direct rates of soot surface oxidation by O_2 were small compared to soot surface oxidation by OH, based on estimated soot surface oxidation rates by O_2 due to Nagle and Strickland-Constable (1960), because soot surface oxidation was completed near the flame sheet where maximum soot concentrations were generally smaller than 1% by volume for present test conditions.

Nomenclature

C_i	=	mass of carbon oxidized per mole of species i reacted (kg kgmol^{-1})
d_p	=	mean primary soot particle diameter (m)
f_s	=	soot volume fraction (-)
[i]	=	molar concentration of species i (kgmol m^{-3})
k	=	Boltzmann constant (J molecule^{-1}K^{-1})
m_i	=	mass of a molecule of species i (kg molecule^{-1})
R_i	=	terms of the HACA soot surface growth rate formulas (kg m^{-2}s^{-1})
S	=	soot surface area per unit volume (m^{-1})
t	=	time (s)
T	=	temperature (K)
u	=	streamwise velocity (ms^{-1})
$\bar{v}_i$	=	mean molecular velocity of species i (ms^{-1})
w_g	=	soot surface growth rate (kg m^{-2}s^{-1})
w_{ox}	=	soot surface oxidation rate (kg m^{-2}s^{-1})
z	=	streamwise distance (m)
α_i	=	empirical (steric) factors in the HACA soot surface growth rate formulas
η_i	=	collision efficiency for soot surface oxidation of species i
ρ,ρ_s	=	gas and soot densities (kg m^{-3})
ϕ	=	fuel-equivalence ratio (-)

Subscripts

CH	=	HACA soot surface growth mechanism of Colket and Hall[11]

---

*Research Scholar, Department of Aerospace Engineering.
†Research Associate, Department of Aerospace Engineering; now Assistant Professor, Department of Mechanical, Materials and Aerospace Engineering, Central Florida University, Orlando, Florida.
**A.B. Modine Professor, Department of Aerospace Engineering; Fellow, AIAA.

FW = HACA soot surface growth mechanism of Frenklach and coworkers[8-10]
o = burner exit condition

INTRODUCTION

The presence of soot is a common feature of nonpremixed (diffusion) flames fueled with hydrocarbons, affecting their structure and reaction mechanisms. As a result, soot processes affect capabilities for computa-tional combustion due to the complexities of soot chemistry, public health due to emissions of particulate soot, fire safety due to increased fire growth rates caused by soot radiation, and combustor durability due to undesirable heat loads caused by continuum radiation from soot. Motivated by these observations, the present investigation sought to extend past work on soot surface growth in laminar premixed and diffusion flames in this laboratory, see Refs. 1-7, seeking to gain a better understanding of effects of fuel type on flame structure and the mechanisms of soot surface growth and oxidation of laminar coflowing jet diffusion flames at atmospheric pressure with the reactants at normal temperature.

Sunderland and coworkers[1-3] experimentally studied the structure and soot surface growth properties of laminar hydrocarbon-air diffu-sion flames by making direct measurements of soot residence times, soot concentrations, soot structure, gas temperatures, and the concentrations of stable gas species. It was found that soot surface growth only occurred when acetylene was present and that growth rates were roughly first-order with respect to acetylene concentrations. Existing detailed soot surface growth models,[8-11] however, could not be evaluated using these results because radical species concentrations important for these mechanisms were not measured.

Xu et al.[4-6] extended Sunderland and coworkers[1-3] by considering soot surface growth in premixed flames. Experimental methods were similar to Sunderland and coworkers[1-3] except that concentrations of radical species (H, OH and O) were determined both computationally and experimentally. It was found that concen-trations of H closely approximated equilibrium requirements in the relatively slowly evolving soot growth regions of premixed flames. The new measurements were then used to evaluate the existing Hydrogen-Abstraction/Carbon-Addition (HACA) soot surface growth mechanisms of Frenklach and coworkers[8-10] and Colket and Hall,[11] finding that the HACA soot growth mechanisms yielded excellent correlations of the measurements soot surface growth rates for quite reasonable values of the steric factors that appear in the theories.

Xu and Faeth[7] continued study of soot surface growth by considering diffusion flame environments that are more relevant to practical soot formation processes in flames. These experiments involved acetylene/air laminar coflowing jet diffusion flames using the full suite of measurements developed during the earlier studies of premixed flames, e.g., Refs. 4-6. These results showed that H concentrations ranged from near-equilibrium conditions to super-equilibrium ratios of 20-30 in the soot surface growth region of the diffusion flames, that soot surface growth rates in premixed flames and diffusion flames satisfy similar reaction rate expressions, and that soot surface growth rates in the diffusion flames were well represented by the HACA mechanisms of Refs. 8-11, with steric factors essentially unchanged from observations in premixed flames.

Soot surface oxidation in premixed and diffusion flame environments must also be understood if reliable predictions of soot emissions from combustion processes are to be made. In addition, soot formation and oxidation generally proceed at the same time in both premixed and diffusion flame environments so that soot surface oxidation rates must be estimated reliably in order to obtain reliable estimates of soot surface growth rates.[1-7] Potential soot oxidants in flames include O_2, CO_2, H_2O, O and OH and numerous simplified treatments can be used to estimate soot surface oxidation rates when only the concentrations of the stable species, O_2, CO_2 and H_2O, are known.[12-17] Recent work, however, has concentrated on more fundamental mechanisms of soot surface oxidation, finding that soot surface oxidation by O_2, CO_2, H_2O and O were relatively unimportant in premixed flame environ-ments but could be described by reaction with OH, see Neoh and coworkers.[18-20] Subsequent studies of soot surface oxidation in diffusion flames due to Garo et al.,[21-22], Puri et al.[23,24] and Haudiquert et al.,[25] however, did not find OH collision efficiencies in good agreement with the findings of Neoh and coworkers[18-20] in premixed flames. One

explanation for these discrepancies is that the optical scattering and extinction measurements that were used to infer soot structure properties during the diffusion flame studies were based on models that have not been very successful for representing the optical properties of soot in flame environments, see Neoh et al.[19] and Koylu and Faeth.[26] Supporting this view is that the use of similar methods during early studies of soot surface growth in fuel-rich premixed flames also proved to be problematical, see the discussion of this point in Xu et al.[4,5] and references cited therein. Whatever the source of the prob-lem, however, these differences between observations of soot surface oxidation rates in premixed and diffusion flames obviously must be resolved.

Based on this status, the present investigation sought to better understand the structure and soot surface growth properties of laminar jet diffusion flames fueled by hydrocarbons other than acetylene that were not directly involved in the HACA soot surface growth mechanism, e.g., ethylene, propylene, propane and benzene. In particular, benzene was considered in order to study the behavior of fuels more closely related to Polycyclic Aromatic Hydro-carbons (PAH) than the other fuels that were studied because PAH soot surface growth mechanisms have been considered to be a potential alternative to HACA soot surface growth mechanisms, see Howard[27] and Richter and Howard.[28] The present measurements also provided information about soot surface oxidation rates which was used to gain a better understanding of soot surface oxidation in flame environments and to improve corrections of measured soot surface growth rates for effects of soot surface oxidation compared to earlier work in this laboratory, e.g., Refs. 4-7. The following description of the research is relatively brief, Xu[29] and El-Leathy[30] should be consulted for more details and complete tabulations of data.

EXPERIMENTAL METHODS

Experimental methods were unchanged from Xu and Faeth,[7] with the same burner arrangement used to observe soot processes in laminar diffusion flames and to calibrate the H concentration measurements using a laminar premixed flame. The burner had a 34.8 mm diameter inner port for the fuel stream flow of the diffusion flames and for the methane-oxygen-nitrogen reactant mixture flow for the premixed flame. A 60 mm diameter coannular outer port was used for the air coflow of the diffusion flames and for the nitrogen coflow of the premixed calibration flame. The air coflow of the diffusion flames served to eliminate natural convection instabilities whereas the nitrogen coflow of the premixed flame served to eliminate the annular diffusion flame for this fuel-rich flame in order to improve the accuracy of the H concentration calibration.

Burner gas flow rates were measured with rotameters. Mixtures were allowed to mix within feed lines that were at least 1000 diameters long to ensure that they were uniform. The flames burned in room air with room disturbances controlled by surrounding them with several layers of screens and a plastic enclosure. The burner could be moved horizontally and vertically with linear positioners in order to accom-modate rigidly-mounted optical instrumen-tation.

Instrumentation

Present measurements were similar to Xu and Faeth[7] and included the following properties measured along the axes of the flames: soot volume fractions, flame tem-peratures, concentrations of major stable gas species, soot structure, gas velocities and concentrations of some radical species (H, OH and O).

Soot volume fractions were measured by deconvoluting laser extinction measure-ments at 632.8 nm for chord-like paths through the flames. Data was reduced using the refractive indices of Dalzell and Sarofim,[31] similar to past work;[1-7] these values have recently been confirmed by Krishnan et al.[32] The experimental uncer-tainties (95% confidence) of soot volume fractions are estimated to be smaller than 10% for soot volume fractions greater than 0.02 ppm, increasing inversely proportional to the soot volume fraction for smaller values.

Soot and gas temperatures are essentially the same;[7] thus soot (gas) temperatures were measured by deconvoluting spectral radia-tion intensities for chord-like paths through the flames and computing temperatures at several wavelength pairs (550/700, 550/750, 550/830, 600/700, 600/750, 600/830 and 650/750 nm). Temperature differences between the average and any of the line pairs were less than 50-100 K and

experimental uncertainties (95% confidence) of these measurements were less than 50 K.

Concentrations of major gas species (N_2, H_2O, H_2, O_2, CO, CO_2, CH_4, C_2H_2, C_2H_4, C_2H_6, C_3H_6, C_3H_8, C_6H_6 and neon, (the last being a tracer gas used to estimate effects of radial diffusion of lithium-containing species that were used to find H concentrations) were measured by sampling and analysis by gas chromatography. Experimental uncertain-ties (95% confidence) of these measure-ments are mainly due to calibration uncertainties and are estimated to be less than 5% for all species concentrations reported here.

Soot structure measurements were limited to primary soot particle diameters carried out by thermophoretic sampling and analysis using Transmission Electron Microscopy (TEM), following Dobbins and Megaridis,[32] similar to earlier work in this laboratory.[26] Primary particle diameters were nearly monodisperse at given positions in each flame (standard deviations were less than 10%) and the experimental uncertainties (95% confidence) of soot primary particle diameter measurements are estimated to be less than 10%.

Streamwise gas velocities were measured using laser velocimetry (LV) with experi-mental uncertainties (95% confidence) less than 5%.

Measurements of H concentrations were carried out by deconvoluted absorption following the Li/LiOH atomic absorption technique of Neoh and coworkers.[18-20] Correction for the radial diffusion of LiOH seed was found from measurements of the concentrations of neon seed, assuming that the diffusivities of LiOH and neon were similar. The H concentration measurements were calibrated using a premixed flame as discussed by Xu and Faeth[6] and similar to Neoh and coworkers.[18-20] Measurements with different seeding levels showed that effects of the LiOH seed on flame properties were negligible, similar to past work.[6,7] Experimental uncertainties (95% confi-dence) of the H concentration measurements are estimated to be smaller than 30%.

Test Conditions

The properties of the laminar premixed flame used to calibrate the H concentration measurements are reported by Xu and Faeth.[6] The data base from the present diffusion flames was extended to include the earlier acetylene-fueled diffusion flame results of Xu and Faeth[7] in order to more completely assess effects of fuel type on diffusion flame structure and soot surface growth and oxidation rate properties. Test conditions for all the diffusion flames considered during the present study are summarized in Table 1. The diffusion flames considered included acetylene-nitrogen, ethylene, propylene-nitrogen, propane and benzene-acetylene-nitrogen fuel streams burning in coflowing air at atmospheric pressure with the reactants at normal temperature. Nitrogen dilution of the fuel stream was used for some of the flames in order to keep maximum soot volume fractions smaller than 2 ppm so that problems of large soot concentrations on the measurements could be avoided. Stoi-chiometric flame lengths (the vertical height of the position along the axis where the local fuel-equivalence ratio was stoichiometric) were 54-130 mm, whereas luminous flame lengths (due to yellow light emitted from heated soot particles) were 80-103 mm. All the flames were well attached, stationary and laminar over the region where measurements were made.

RESULTS AND DISCUSSION

Soot Structure

A TEM photograph of soot particles along the axis of the ethylene/air flame (Flame 4), obtained near the end of the soot formation region where the soot volume fraction is a maximum, is illustrated in Fig. 1. Soot particle images at other locations and for other flames are qualitatively the same and were generally similar to TEM images of soot particles obtained in other premixed and diffusion flames that have been studied, see Refs. 1-7 and references cited therein. In general, soot particles consist of roughly spherical primary soot particles that have nearly constant diameters at a particular flame condition, collected into aggregates that are known to be mass fractal objects.[26,32] The mean number of primary soot particles per aggregate increased with increasing distance from the burner exit, similar to the measurements of this property due to Sunderland et al.[1]

Flame Structure

Measurements of gas (soot) temperatures, streamwise gas velocities, soot volume fractions,

primary soot particle diameters, concentrations of major gas species and concentrations of radical species (H, OH and O) are plotted as a function of the distance along the flame axis for an acetylene/air flame (Flame 1), the ethylene/air flame (Flame 4) and a benzene-acetylene/air flame (Flame 8) in Figs. 2-4. Corresponding residence times, found by integrating the velocity measurements, are indicated at the top of the plots. The residence times are relative to the first position where detectable soot volume fractions were observed (at z = 10-20 mm for the three flames). The stoichiometric (ϕ=1), or flame sheet condition for the three flames occurs at z = 54, 81 and 130 mm, with the last lying beyond the region that is illustrated in Fig. 4. Luminous flame lengths coincide with the right hand boundaries of the figures for all three flames, although soot concentrations near these boundaries were too small to be accurately measured and reported using present methods.

Gas (soot) temperatures along the flame axes in Figs. 2-4 reach a maximum well before the maximum soot concentration and flame sheet conditions are reached. This behavior is similar to other soot-containing laminar jet diffusion flames that have been studied in this laboratory and is caused by continuum radiation heat losses from soot.[1-3,7]

Gas velocities along the flame axes in Figs. 2-4 increase from burner exit values smaller than 0.1 m/s to values in excess of 2 m/s at the highest positions that were measured. These velocity increases were caused by effects of buoyancy due to the relatively small flame densities and burner exit velocities of the test flames.

Similar to earlier observations of soot-containing laminar jet diffusion flames in this laboratory, Refs. 1-3, and 7, primary soot particle diameters reach maximum values relatively early in the soot formation region. This behavior is caused by accelerating primary soot particle nucleation rates with increasing streamwise distance in the initial portions of the soot formation region, which is caused by progressively increasing H concentrations with increasing streamwise distance, see Xu and Faeth.[7] This behavior causes the relatively few primary soot particles formed near soot inception conditions, that become large due to long periods of soot surface growth, to be superseded by the much larger number of primary soot particles formed later in the soot formation region that are smaller due to shorter periods of soot surface growth. This behavior is aided by the fact that rates of soot surface growth remain relatively rapid near soot inception conditions, as noted by Tesner,[34,35] which allows the relatively few primary particles present there to grow quite large.

Significant levels of soot formation (evidenced by the appearance of measurable soot concentrations), were generally asso-ciated with the first streamwise locations where detectable concentrations of both acetylene and H were observed, similar to the observations of Figs. 2-4. Soot formation (as indicated by soot surface growth) became small again where maximum soot volume fractions were reached; which occurred in the presence of relatively large concentrations of H but where acetylene concentrations became smaller than roughly 1% by volume. This behavior was also similar to other soot-containing laminar jet diffusion flames that have been studied in this laboratory, see Refs. 1-3 and 7. An interesting feature of conditions where soot formation again became small in flames involving benzene as a portion of the fuel, see Fig. 4, was that this event was definitely correlated with concentrations of acetylene becoming small, whereas concentrations of benzene remained relatively constant in this region.

The concentrations of major stable gas species in Figs. 2-4 are similar to concentrations of major stable gas species in other laminar flames burning in air, involving acetylene and other hydrocarbons as fuels, see Refs. 1-3. If the original fuel is not acetylene, decomposition of the original fuel yields significant concentrations of acetylene relatively near the burner exit. As a result, concentrations of acetylene within flames fueled by hydrocarbons other than acetylene are generally quite similar to acetylene concentrations within acety-lene/air flames, compare Figs. 2-4. Thus, concentrations of the hydrocarbon fuels decrease and O_2 concentrations increase with increasing distance within the soot formation region, whereas intermediate hydrocarbons — CH_4, C_2H_2 (when not the fuel), C_2H_4 (when not the fuel) and C_2H_6 — reach a maximum somewhat before the location where soot concentrations reach a maximum. The final combustion products, CO_2 and H_2O, increase

throughout the soot formation region, reaching broad maxima near the flame sheet (ϕ=1). Intermediate combustion products, associated with water-gas equilibrium, e.g., CO and H_2, are present in relatively large concentrations throughout the soot formation region, reaching broad maxima somewhat upstream of the flame sheet. Finally, nitrogen concentrations remain relatively uniform for the flame regions illustrated in Figs. 2-4.

Concentrations of H, OH and O all increase monotonically as the flame sheet is approached. Near-equilibrium concentra-tions were observed near the onset of soot formation, but H and OH concentrations eventually become 10-20 times larger than equilibrium concentrations near the flame sheet. Concentrations of O exhibit even larger superequilibrium ratios; nevertheless, O concentrations generally are 100-1000 times smaller than H and OH concentrations throughout most of the region where soot is present.

The region where soot is present in Figs. 2-4 contains significant concentrations of species potentially responsible for soot oxidation, e.g., O_2, CO_2, H_2O, O and OH.[12-20] In particular, O_2 is invariably present at concentrations on the order of 0.1% (by volume) throughout most of the soot surface growth region of laminar coflowing jet diffusion flames.[1-3,7] Similar concentrations of O_2 are also observed in the fuel-rich regions of opposed-jet diffusion flames;[36] therefore, this effect does not appear to be due to O_2 leakage through the base of coflowing jet diffusion flames. Thus, soot formation and oxidation proceed at the same time, with soot formation dominating the process up to the maximum soot volume fraction condition and soot oxidation dominating the process thereafter.

Soot Surface Reaction Rate Properties

Past and present measurements of laminar premixed and diffusion flames were used to study soot surface growth and oxidation similar to earlier studies based on laminar flames.[1-7] Major assumptions were identical to the earlier work, as follows: soot surface growth, rather than soot nucleation, dominates soot mass production; soot surface oxidation dominates soot oxidation; effects of diffusion (Brownian motion) and thermophoresis on soot motion are small, so that soot particles convect along the axes of the flames at the local gas velocity; the soot density is constant; and the surface area available for soot surface growth and oxidation is equivalent to constant diameter spherical primary soot particles that meet at a point. See Refs. 1-7 for justification of these assumptions.

The first soot formation property of importance is the number of primary particles per unit volume, found from the measured soot volume fractions and primary soot particle diameters, as follows:[1]

$$n_p = 6f_s/(\pi d_p^3) \quad (1)$$

The experimental uncertainties (95% confidence) of n_p are estimated to be less than 32% for $f_s \geq 0.1$ ppm, increasing inversely proportional to f_s for smaller values of f_s. The soot surface area per unit volume is given by the same measurements, as follows:[1]

$$S = 6f_s/d_p \quad (2)$$

The experimental uncertainties (95% confidence) of S are estimated to be less than 16% for $f_s \geq 0.1$ ppm, increasing inversely proportional to f_s for smaller values of f_s. Defining the soot surface growth rate as the rate of increase of soot mass per unit surface area and time, and the soot surface oxidation rate as the rate of decrease of soot mass per unit surface area and time, conservation of soot mass along a streamline under the previous assumptions gives the soot surface growth and oxidation rates, as follows:[1]

$$w_g = -w_{ox} = (\rho/S)d(\rho_s f_s/\rho)/dt \quad (3)$$

where present measurements of species concentrations and temperatures yield the gas density, assuming an ideal gas mixture and the minus sign is inserted so that w_{ox} is a positive number. The temporal derivative in Eq. 3 was found from three-point least-squares fits of the argument of the derivative, similar to past work. The soot density in Eq. 3 was taken to be equal to 1850 kg/m^3, similar to past work.[1-7] Finally, consideration of soot surface oxidation was limited to early soot oxidation (soot mass consumption less than 70%) where problems of soot aggregate breakup, the development of primary soot particle porosity, and internal oxidation of primary soot particles, do not yet occur, see Neoh et al.[20] Estimated experimental uncertainties (95% confidence) of soot surface

growth rates are less than 30%; estimated experimental uncertainties of soot surface oxidation rates are comparable.

Soot Surface Growth Rates

Gross soot surface growth rates for all the premixed and diffusion flames considered during the present investigation were corrected for effects of soot surface oxidation because soot surface growth and oxidation proceed at the same time, as noted in connection with Figs. 2-4. The correction for soot surface oxidation, however, was not done in the same way as past work, e.g., Refs. 1-7; instead, present findings concerning soot surface oxidation in soot-containing flames were used to estimate soot surface oxidation for all the flames. The details of the new results concerning soot surface oxidation will be presented subsequently, the main features of these results are as follows: soot surface oxidation was dominated by the OH oxidation mechanism of Neoh et al.[9] with nearly the same collision efficiency, after allowing for direct soot surface oxidation by O_2 based on the mechanism of Nagle and Strickland-Constable[12] (which was later confirmed by Park and Appleton[13]). It was found that effects of corrected soot surface growth rates in this way were small, except when soot surface growth rates themselves became small toward the end of the soot formation region. Thus, in order to be conservative about potential effects of soot surface oxidation, determination of soot surface growth rates, corrected for effects of soot surface oxidation, were limited to conditions where estimated soot surface oxidation rates never exceeded half the gross soot growth rates, similar to past work.[1-7]

Present measurements of soot surface growth rates also were baselined with earlier results in laminar premixed and diffusion flames by correcting gross soot surface growth rates for effects of soot surface oxidation in the same manner as earlier studies of soot surface growth in this laboratory.[1-7] In this case, rates of soot surface oxidation were estimated as follows: soot surface oxidation by O and H was ignored, soot surface oxidation by O_2 was based on the results of Nagle and Strickland-Constable,[12] and soot surface oxidation by H_2O and H_2O_2 were estimated following Libby and Blake[14,15] and Johnstone et al.,[16] which gave results similar to Bradley et al.[17] Similar to present estimates of net soot surface growth rates, considering effects of the OH and O_2 soot surface oxidation mechanisms, the results for net soot surface growth rates considering the O_2, CO_2 and H_2O soot surface oxidation mechanism, were limited to conditions where estimated soot oxidation rates never exceeded half the gross soot surface growth rate. As a result of this conservative approach, the net soot surface growth rates found using the O_2 and OH approach were essentially the same as those found using the O_2, CO_2 and H_2O approach.

Soot surface growth rates were interpreted using the HACA soot growth mechanisms of Frenklach and coworkers,[8-10] and Colket and Hall[11] in order to maintain consistency with past evaluations of these mechanisms based on similar measurements and due to the success of these approaches for correlating measurements of soot surface growth in premixed ethylene/air and methane/oxygen flames[4,5] and in acetylene/air diffusion flames.[7] In all cases, net soot surface growth rates were expressed, as follows:

$$w_g = \alpha_i R_i \qquad (4)$$

where i = FW or CH denotes reaction parameters for the HACA soot surface growth rate mechanisms of Frenklach and coworkers,[8-10] and Colket and Hall[11] which were found from the measurements. The details of these mechanisms, the formulas for the R_i, and the reaction-rate parameters for the R_i can be found in Xu et al.[4] The parameters, α_i are empirical steric factors on order of unity, with α_{FW} specified to be a function of temperature,[8-10] and α_{CH} specified to be a constant.[11]

As a first approximation for all the premixed and diffusion flames considered during this study, the R_i are proportional to the product $[H][C_2H_2]$. Thus, values of $w_g/[C_2H_2]$ measured for all the studies were plotted as a function of [H] to provide a direct test of the main features of the HACA soot surface growth mechanisms without the intrusion of uncertainties due to the numerous empirical parameters of the detailed HACA mechanisms of Refs. 8-11. A plot of this type, including all soot surface growth rate measurements except the present measurements involving diffusion flames fueled with hydrocarbons other than acetylene, is provided in

Xu and Faeth.[7] Adding present measurements and changing the correction for soot surface oxidation does not materially affect the correlation between w_g and the product $[C_2H_2][H]$ and supports a first-order relationship between w_g and the concentrations of acetylene and H. Notably, this behavior is also completely consistent with present observations that significant soot formation (growth) is first observed at the location where significant concentrations of both acetylene and H are observed, that soot surface growth ends in the presence of significant concentrations of H when acetylene disappears, and that the end of soot formation is observed when acetylene disappears even though concentrations of benzene are still significant (see Fig. 4).

A more direct evaluation of the HACA mechanisms of soot surface growth is obtained by plotting w_g directly as a function of α_{FW} R_{FW} (after correlating α_{FW} as a function of temperature) for the Frenklach and coworkers[8-10] mechanism, and as a function of R_{CH} for the Colket and Hall[11] mechanism. These results for the Frenklach and coworkers[8-10] mechanism are discussed by El-Leathy;[30] the corresponding results for the Colket and Hall[11] mechanism are illustrated in Fig. 5. In this figure, available measurements for both premixed and diffusion flames (after correcting all measurements for soot surface oxidation based on the present measurements) are illustrated along with best-fit correlation for all the flames. The corresponding steric factor and its experimental uncertainties (95% confidence) is 1.0 with an uncertainty of 0.2. First of all, it is encouraging that the steric factor is of order of magnitude unity, as expected.[11] Next, the use of the Colket and Hall[11] HACA mechanism improves the correlation of soot surface growth rates solely in terms of the approximate correlation based on only the leading terms of the HACA mechanisms, appearing in Xu and Faeth.[7] The correlation for the diffusion flames and all the flames is essentially the same. Correlated values of soot surface growth rates for the premixed flames are slightly lower than for the diffusion flames (possibly because estimates of H concentrations are based on the assumption of local equilibrium of H, which is somewhat larger than the measurements, were used for the premixed flames) but the differences are comparable to present experimental uncertainties. Considering the results for the diffusion flames alone, there clearly is no difference between estimates of w_g based on the HACA mechanisms as the hydrocarbon fuel type is varied. This includes flames with and without benzene present, even though benzene is more closely related to PAH than the other fuels that were considered and might be thought to potentially enhance channels of soot surface growth by the PAH mechanism compared to the HACA mechanism, see Howard.[27] The behavior using the HACA mechanism of Frenklach and coworkers[8-10] see El-Leathy,[30] is essentially the same. Naturally, these findings are also consistent with the onset of soot formation occurring when [H] first appears in the presence of significant acetylene concentrations on the burner side of the soot formation region and the end of soot formation occurring when acetylene subsequently disappears in the presence of significant H and benzene concentrations on the flame sheet side of the soot formation region.

Similar to earlier findings for soot surface growth rates,[4,5,7] the HACA soot surface growth rate mechanisms of Frenklach and coworkers[8-10] and Colket and Hall[11] continue to be encouraging and they may eventually provide the basis of reliable methods to estimate soot surface growth rates in flame environments fueled with hydrocarbons. Uncertainties remain, however, about effects of pressure, about behavior at higher temperatures than considered thus far, and about effects of PAH as fuels, on soot surface growth rates.

Soot Surface Oxidation Rates

Present measurements of soot surface oxidation rates were corrected for effects of soot surface growth based on the Colket and Hall[11] soot surface growth mechanism, correlated as just described. No condition is considered in the following, however, where the correction for soot surface growth was more than half the gross soot surface oxidation rate.

Similar to Neoh et al.,[19] present soot surface oxidation rates (corrected for soot surface growth) were converted into collision efficiencies based on kinetic theory estimates of the collision rates of a given gas species with the surface of primary soot particles. Thus, the collision efficiency for a potential oxidizing species is given by the following expression:[2]

$$\eta_i = 4w_{ox}/(C_i[i]\bar{v}_i) \quad (5)$$

where C_i is the mass of carbon removed from the surface per mole of species i reacting at the surface, [i] is the gas phase concentration of i adjacent to the surface, and

$$\bar{v}_i = (8kT/(\pi m_i))^{1/2} \quad (6)$$

is the (Boltzmann) equilibrium mean molecular velocity of species i. Values of η_i were measured for potential soot surface oxidation for i = O_2, CO_2, H_2O, O and OH.

The collision efficiencies of O_2 for soot surface oxidation are plotted as a function of height above the burner in Fig. 6. Results shown on the figure include the range of values observed by Neoh et al.[19] in premixed flames, the values measured by Xu and Faeth[7] and the present investigation in diffusion flames, and values estimated from the predictions of Nagle and Strickland-Constable[12] for conditions in the diffusion flames considered by Xu and Faeth[7] and the present investigation. The Nagle and Strickland-Constable[12] approach has exhib-ited effective capabilities to predict soot surface oxidation by O_2, see Park and Appleton[13] and references cited therein, and there are significant concentrations of O_2 for soot paths along the axes of the diffusion flames, see Figs. 2-4. Thus, the fact that the Nagle and Strickland-Constable[12] estimates of the O_2 collision efficiency are 10-100 times smaller than the measurements in diffusion flames, strongly suggests that some other species is mainly responsible for soot surface oxidation in the diffusion flames. Other evidence that O_2 is not the main direct oxidizing species for flame environments is provided by the large scatter (nearly a factor of 100) of the collision efficiencies for the diffusion flames, combined with the even larger scatter (more than a factor of 100) of the collision efficiencies of Neoh et al.[19] for premixed flames.

The collision efficiencies of H_2O for soot surface oxidation are plotted as a function of height above the burner in Fig. 7. Results shown on the figure include the range of values reported by Neoh et al.[19] for premixed flames, and values from the diffusion flames both considering and ignoring the contribution of oxidation by O_2 (the latter estimated using the Nagle and Strickland-Constable[12] correlation). First of all, it is evident that allowing for direct oxidation by O_2 generally has a small effect on the collision efficiencies in diffusion flames illustrated in Fig. 7. In addition, there is significant scatter (roughly a factor of 100) of the collision efficiencies in diffusion flames and a comparable scatter (roughly a factor of 100) of the collision efficiencies of Neoh et al.[19] in premixed flames. These findings, clearly do not support H_2O as a major direct contributor to soot surface oxidation in flames, either alone or in parallel with soot oxidation by O_2. Consideration of soot surface oxidation by CO_2 and O yielded similar conclusions, see El-Leathy.[30]

Finally, the collision efficiencies of OH for soot surface oxidation are plotted as a function of height above the burner in Fig. 8, in the same manner as the results for H_2O in Fig. 7. With perhaps one exception (at an extreme condition where experimental uncertainties are relatively large), direct O_2 surface oxidation of soot is not very important for these conditions, as before. On the other hand, similar to the observations of Neoh et al.,[19] collision efficiencies for OH for the diffusion flames exhibit relatively small degrees of scatter (roughly a factor of 3) and are in excellent agreement with the results of Neoh et al.[19] for premixed flames. In particular, the mean collision efficiency of OH for soot surface oxidation in the diffusion flames is 0.10 with a standard deviation of 0.07 which is in excellent agreement with the value of 0.13 found by Neoh et al.[19] for soot surface oxidation in premixed flames using the same treatment of soot structure as the present investigation. Finally, this agreement was achieved over a relatively broad range of flame conditions for the combined results in premixed and diffusion flames as follows: temperatures of 1570-1870 K, oxygen mole fractions of 1×10^{-5} – 1.2×10^{-2}, and levels of soot mass consumption less than 70% at atmospheric pressure for flames fueled with a variety of fuels. Although these results are helpful, however, the properties of the final stage of oxidation, where internal oxidation of primary soot particles becomes a factor, effects of pressure on soot oxidation, and possibly effects of fuel type on soot oxidation for hydrocarbons other than those considered here, all merit additional study in the future.

CONCLUSIONS

Flame structure and soot surface growth and oxidation rates were studied for coflowing laminar jet diffusion flames. Present experimental measurements were supplemented by the earlier findings of Xu and Faeth[7] so that the complete data base involved acetylene, ethylene, propylene, propane and benzene-acetylene/air flames burning at atmospheric pressure with the reactants at normal temperature as summarized in Table 1. This information about soot surface growth rates in diffusion flames was also supplemented by earlier measurements in premixed ethylene/air and methane/oxygen flames due to Xu et al.[4,5] which also involved flames at atmospheric pressure with the reactants at normal temperature. The major conclusions of the study are as follows:

1. In all flames that were considered, the original fuel decomposes relatively early during the soot formation process, yielding species generally associated with soot surface growth and oxidation, e.g., C_2H_2, H and OH, among others. The yields of these species are affected by flame type (premixed or diffusion flame), fuel species and flame operating conditions (e.g., nitrogen concentration in the fuel stream), however, subsequent reaction of these species during processes of soot surface growth and oxidation are largely dependent on local flame conditions and are not materially affected by either the fuel type or whether these processes are occurring in premixed or diffusion flame environments.

2. Soot surface growth rates in laminar diffusion and premixed flames, for various fuel types in both types of flames, agree within experimental uncertainties at comparable local conditions and could be correlated reasonably well by the HACA soot surface growth mechanisms of Frenklach and coworkers[8-10] and Colket and Hall,[11] with steric factors in both these mechanisms having values on the order of unity, as expected.

3. Soot surface oxidation rates in the laminar diffusion flames, for various fuel types, could be correlated by assuming a constant collision efficiency for OH for soot surface oxidation of 0.10 with a standard deviation of 0.07. This finding is in good agreement with the OH collision efficiency for soot surface oxidation of 0.13 for assumed similar soot structure properties found by Neoh et al.[19] for measurements in premixed flames at atmospheric pressure at similar O_2 concentrations. The correction of present soot surface oxidation rates for oxidation by O_2 based on the results of Nagle and Strickland-Constable[12] was small (on average less than 10%) compared to soot surface oxidation by OH for present conditions.

4. Current findings concerning soot surface oxidation rates in diffusion flames were used to correct gross measurements of soot surface growth rates for simultaneous effects of soot surface oxidation. This approach involved estimating soot surface oxidation rates by O_2 based on the results of Nagle and Strickland-Constable[12] and by OH as proposed by Neoh et al.[19] but using the present OH collision efficiency. Corrected soot surface growth rates were only considered in cases where estimated soot surface oxidation rates were less than half the gross soot surface growth rates for all flames considered here, which was the same as the approach used during earlier studies when other mechanisms of soot surface oxidation were considered.[4,5,7] Due to this relatively conservative approach for correcting soot surface growth rates for effects of soot surface oxidation, however, present estimates of net soot surface growth rates were essentially unchanged from earlier results, e.g., Refs. 4,5 and 7.

It should be recalled that all the results considered here involved flames at atmos-pheric pressure, fueled with a limited number of hydrocarbons, and with the reactants initially at normal temperature; applications of these results to other flame conditions should be approached with caution.

ACKNOWLEDGMENTS

This research was sponsored by NASA Grants NCC3-661, NAG3-1878, NAG3-2048 and NAG3-2404 under the technical management of D. L. Urban and Z.-G. Yuan of the NASA Glenn Research Center.

REFERENCES

[1]Sunderland, P.B., Köylü, Ü.Ö., and Faeth, G.M., "Soot Formation in Weakly Buoyant Acetylene-Fueled Laminar Jet Diffusion Flames Burning in

Air," *Combustion and Flame*, Vol. 100, Nos. 1/2, 1995, pp. 310-322.

[2]Sunderland, P.B., and Faeth, G.M., "Soot Formation in Hydrocarbon/Air Laminar Jet Diffusion Flames," *Combustion and Flame*, Vol. 105, Nos. 1/2, 1996, pp. 132-146.

[3]Lin, K.-C., Sunderland, P.B., and Faeth, G.M., "Soot Nucleation and Growth in Acetylene/Air Laminar Coflowing Jet Diffusion Flames," *Combustion and Flame*, Vol. 104, No. 3, 1995, pp. 369-375, 1996.

[4]Xu, F., Sunderland, P.B., and Faeth, G.M., "Soot Formation in Laminar Premixed Methane/Oxygen Flames at Atmospheric Pressure," *Combustion and Flame*, Vol. 108, No. 4, 1997, pp. 471-493.

[5]Xu, F., Lin, K.-C., and Faeth, G.M. "Soot Formation in Laminar Premixed Methane/Oxygen Flames at Atmospheric Pressure," *Combustion and Flame*, Vol. 115, Nos. 1/2, 1998, pp. 195-209.

[6]Xu, F., and Faeth, G.M., "Structure of the Soot Growth Region of Laminar Premixed Methane/Oxygen Flames," *Combustion and Flame*, Vol. 121, No. 4, 2000, pp. 640-650

[7]Xu, F., and Faeth, G.M. "Soot Formation in Laminar Acetylene/Air Diffusion Flames at Atmospheric Pressure," *Combustion and Flame*, Vol. 125, Nos. 1/2, 2001, pp. 804-819.

[8]Frenklach, M., and Wang, H. "Detailed Modeling of Soot Particle Nucleation and Growth," *Proceedings of the Combustion Institute*, Vol. 23, 1990, pp. 1559-1556.

[9]Frenklach, M., and Wang, H., *Soot Formation in Combustion* (H. Bockhorn, ed.), Springer-Verlag, Berlin, 1994, pp. 165-192.

[10]Kazakov, A.,Wang, H., and Frenklach, M., "Detailed Modeling of Soot Formation in Laminar Premixed Ethylene Flames at a Pressure of 10 Bar," *Combustion and Flame*, Vol. 100, Nos. 1/2, 1995, pp. 111-120.

[11]Colket, M.B., and Hall, R.J., "Successes and Uncertainties in Modelling Soot Formation in Laminar Premixed Flames," *Soot Formation in Combustion* (H. Bockhorn, ed.), Springer-Verlag, Berlin, 1994, pp. 442-470.

[12]Nagle, J., and Strickland-Constable, R.F., "Oxidation of Carbon Between 1000-2000°C," *Proceedings of Fifth Carbon Conference*, Vol. 1, 1962, pp. 154-164.

[13]Park, C., and Appleton, J.P., "Shock-Tube Measurements of Soot Oxidation Rates," *Combustion and Flame,* Vol. 20, No. 3,1973, pp. 369-379.

[14]Libby, P.A., and Blake, T.R., "Theoretical Study of Burning of Carbon Particles," *Combustion and Flame*, Vol. 36, No. 2,1979, pp. 139-169.

[15]Libby, P.A., and Blake, T.R., "Burning of Carbon Particles in the Presence of Water Vapor," *Combustion and Flame*, Vol. 41, No. 2, 1981, pp. 123-147.

[16]Johnstone, J.F., Chen, C.Y., and Scott, D.S., "Kinetics of the Steam-Carbon Reaction in Porous Graphite," *Industrial Engineering Chemistry*, Vol. 44, 1952, pp. 1564-1569.

[17]Bradley, D., Dixon-Lewis, G., El-Din Habik, S., and Mushi, E.M.J., "The Oxidation of Graphite Powder in Flame Reaction Zones," *Proceedings of the Combustion Institute*, Vol. 20, 1984, pp. 931-940.

[18]Neoh, K.G., *Soot Burnout in Flames*, Ph.D. Thesis, Massachusetts Institute of Technology, Cambridge, MA, 1980.

[19]Neoh, K.G., Howard, J.B., and Sarofim, A.F., "Soot Oxidation in Flames," *Particulate Carbon* (D.C. Siegla and B.W. Smith, ed.), Plenum Press, New York, 1980, pp. 261-277.

[20]Neoh, K.G., Howard, J.B., and Sarofim, A.F., "Effect of Oxidation on the Physical Structure of Soot," *Proceedings of the Combustion Institute*, Vol. 20, 1984, pp. 951-957.

[21]Garo, A., Lahaye, J., and Prado, G., "Mechanisms of Formation and Destruction of Soot Particles in a Laminar Methane-Air Diffusion Flame," *Proceedings of the Combustion Institute*, Vol. 21, 1986, pp. 1023-1031.

[22]Garo, A., Prado, G., and Lahaye, J., "Chemical Aspects of Soot Particles Oxidation in a Laminar Methane-Air Diffusion Flame," *Combustion and Flame*, Vol. 79, Nos. 3 and 4, 1990, pp. 226-233.

[23]Puri, R., Santoro, R.J., and Smyth, K.C., "The Oxidation of Soot and Carbon Monoxide in Hydrocarbon Diffusion Flames," *Combustion and Flame*, Vol. 97, No. 2, 1994, pp. 125-144 (1994); also, *Ibid.*, Erratum, *Combustion and Flame*, Vol. 102, No. 1/2, 1995, pp. 226-228.

[24]Puri, R., Santoro, R.J., and Smyth, K.C., "The Oxidation of Soot and Carbon Monoxide in Hydrocarbon Diffusion Flames," *Combustion and Flame*, Vol. 102, Nos. 1/2, 1995, pp. 226-228.

[25]Hardiquert, M., Cessou, A., Stepowski, D., and Coppalle, A., "OH and Soot Concentration Measurements in a High-Temperature Laminar Diffusion Flame," *Combustion and Flame*, Vol. 111, No. 4, 1997, pp. 338-349.

[26]Köylü, Ü.Ö., and Faeth, G.M., "Structure of Overfire Soot in Buoyant Turbulent Diffusion Flames at Long Residence Times," *Combustion and Flame*, Vol. 89, No. 2, 1992, pp. 140-156.

[27]Howard, J.B., "Carbon Addition and Oxidation Reactions in Heterogeneous Combustion and Soot Formation," *Proceedings of the Combustion Institute*, Vol. 23, 1990, pp. 1107-1127.

[28]Richter, H. and Howard, J.B.,"Formation of Polycyclic Aromatic Hydrocarbons and Their Growth to Soot — A Review of Chemical Reaction Pathways," *Progress in Energy and Combustion Science*, Vol. 26, Nos. 4-6, 2000, pp. 565-608.

[29]Xu, F., *Soot Growth in Laminar Premixed Flames*, Ph.D. Thesis, The University of Michigan, 1999.

[30]El-Leathy, A.M., *Effects of Fuel Type on Soot Formation and Oxidation in Laminar Diffusion Flames*, Ph.D. Thesis, Mechanical Power Department, Helwan University, Cairo, Egypt, in press.

[31]Dalzell, W.H., and Sarofim, A.F., "Optical Constants of Soot and Their Application to Heat Flux Calculations," *Journal of Heat Transfer*, Vol. 91, No. 1, 1969, pp. 100-104.

[32]Krishnan, S.S., Lin, K.-C., Wu, J.-S., and Faeth, G.M., "Optical Properties in the Visible of Overfire Soot in Large Buoyant Turbulent Diffusion Flames," *Journal of Heat Transfer*, Vol. 122, No. 3, 2000, pp. 517-524.

[33]Dobbins, R.A., and Megaridis, C.M. "Morphology of Flame-Generated Soot as Determined by Thermophoretic Sampling," *Langmuir*, Vol. 3, No. 2, 1987, pp. 254-259.

[34]Tesner, P.A., "Formation of Dispersed Carbon by Thermal Decomposition of Hydrocarbons," *Proceedings of the Combustion Institute*, Vol. 7, 1958, pp. 546-556.

[35]Tesner, P.A., "Dispersed Carbon Formation by Acetylene Self-Combustion," *Proceedings of the Combustion Institute,* Vol. 8, 1960, pp. 627-633.

[36]Lin, K.-C., and Faeth, G.M. "Structure of Laminar Permanently-Blue Opposed-Jet Ethylene-Fueled Diffusion Flames," *Combustion and Flame*, Vol. 115, 1998, pp.468-480.

Table 1. Summary of Laminar Jet Diffusion Flames[a]

FLAME	HC TYPE	HC[c] (%)	C_2H_2[c] (%)	N_2[c] (%)	L_s (mm)	L_v (mm)
1[b]	---	---	16.9	83.1	54	82
2[b]	---	---	15.1	84.9	55	80
3[b]	---	---	17.5	82.5	66	103
4	C_2H_4	100.0	---	---	81	100
5	C_3H_6	18.8	---	81.2	74	100
6	C_3H_8	100.0	---	---	79	100
7	C_6H_6	0.7	14.1	85.2	95	90
8	C_6H_6	1.4	10.2	88.4	130	90
9	C_6H_6	2.3	5.6	92.1	110	90

[a]Round laminar jet diffusion flames with 35 mm ID fuel port and 60 mm ID coflowing air port. Reactant and ambient pressures and temperatures of 98 ± 1 kPa and 294 ± 2 K. Reactant purities: C_2H_2, 99.5%; C_2H_4, 99.0%; C_3H_6, 99.5%; C_3H_8, 99.5%; C_6H_6, 99.5%; N_2, 99.9%; laboratory air coflow having a 240 K dewpoint.
[b]From Xu and Faeth[7], rest from present investigation.
[c]Percent by volume of fuel port flow.

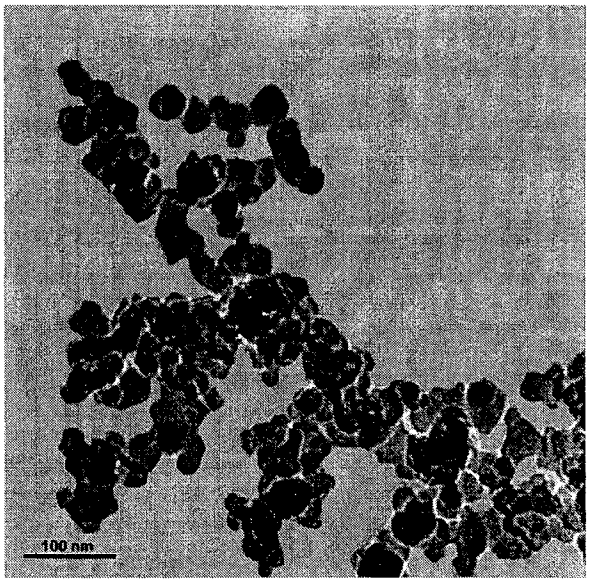

Fig. 1 Typical TEM photograph of soot aggregates at the maximum soot volume fraction location along the axis of the ethylene-fueled laminar jet diffusion flame burning in air at atmospheric pressure with the reactants at normal temperature (Flame 4).

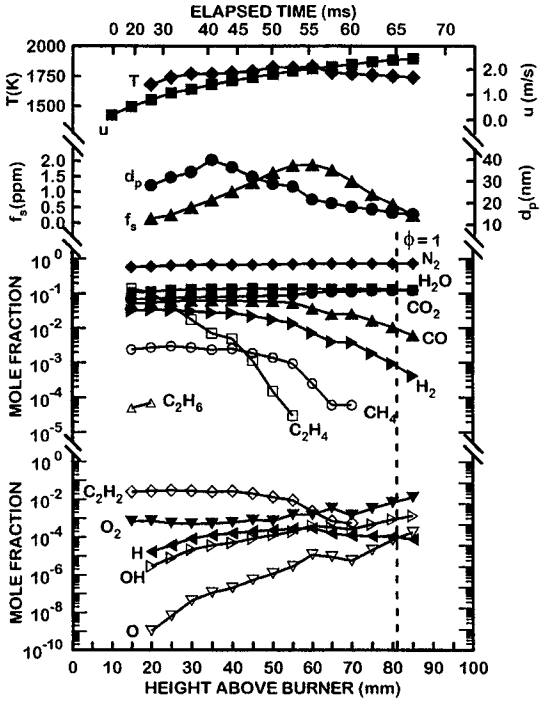

Fig. 3 Measured soot and flame properties along the axis of the ethylene/air laminar jet diffusion flame at atmospheric pressure (Flame 4).

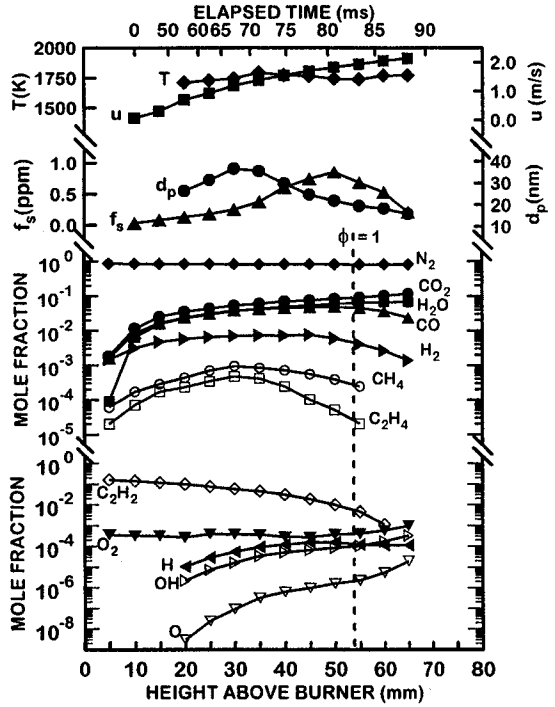

Fig. 2 Measured soot and flame properties along the axis of an acetylene-nitrogen/air laminar jet diffusion flame at atmospheric pressure (Flame 1). From Xu and Faeth.[7]

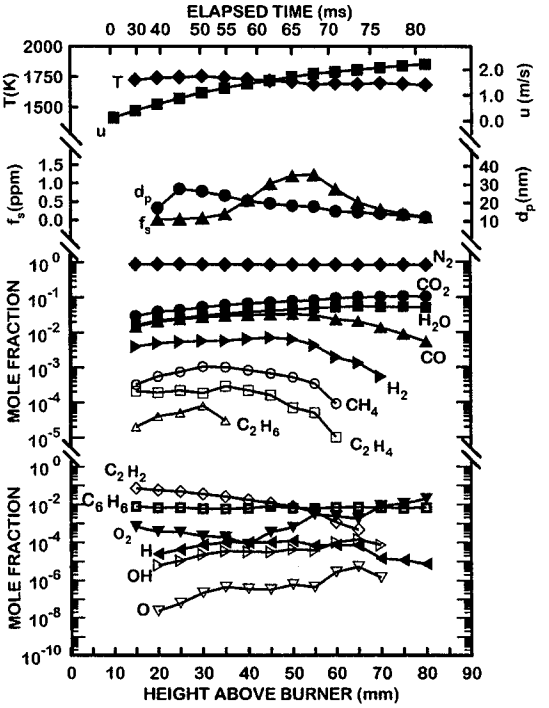

Fig. 4 Measured soot and flame properties along the axis of a benzene-acetylene-nitrogen/air laminar jet diffusion flame at atmospheric pressure (Flame 8).

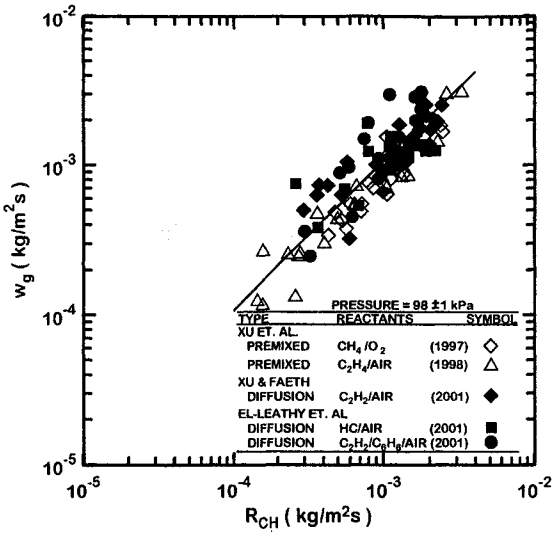

Fig. 5 Soot surface growth rates (corrected for soot surface oxidation) in terms of the HACA mechanism of Colket and Hall[11] for laminar flames at atmospheric pressure. Measurements of ethylene/air premixed flames from Xu et al.;[4] measurements of methane/oxygen premixed flames from Xu et al.;[5] measurements of acetylene-nitrogen/air diffusion flames from Xu and Faeth;[7] and measurements of ethylene/air, propylene-nitrogen/air, propane/air and acetylene-benzene-nitrogen/air diffusion flames from the present investigation.

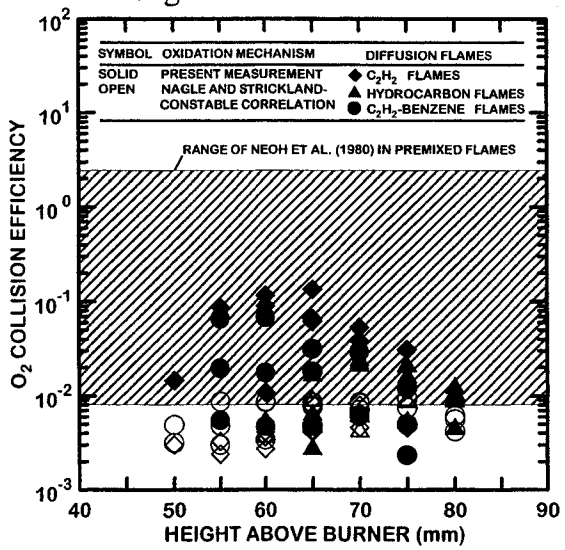

Fig. 6 Soot surface oxidation collision efficiencies assuming soot burnout due to attack by O_2 as a function of height above the burner. Found from the measurements of Neoh et al.[19] in premixed flames, estimated from the correlation for attack by O_2 of Nagle and Strickland-Constable[12] for the conditions of the present diffusion flames, and found from the present measurements in diffusion flames. Note that the data base for the present diffusion flames includes the measurements of Xu and Faeth[7] as well as the present investigation.

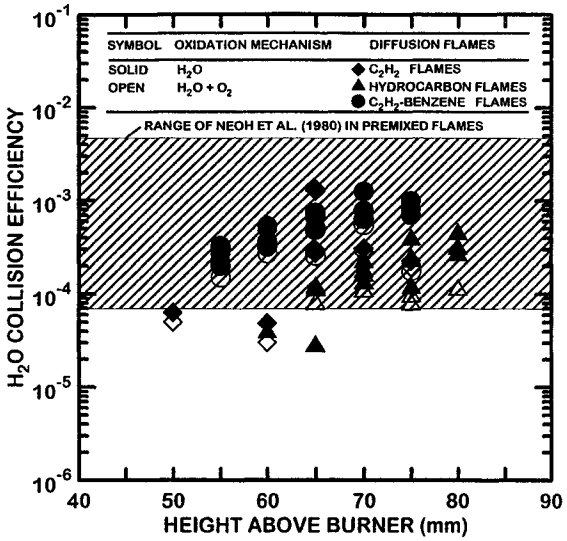

Fig. 7 Soot surface oxidation collision efficiencies assuming soot burnout due to attack by H_2O as a function of height above the burner. Found from the measurements of Neoh et al.[19] in premixed flames, estimated from the correlation for attack by O_2 of Nagle and Strickland-Constable[12] for the conditions of the present diffusion flames, and found from the present measurements in diffusion flames. Note that the data base for the present diffusion flames includes the measurements of Xu and Faeth[7] as well as the present investigation.

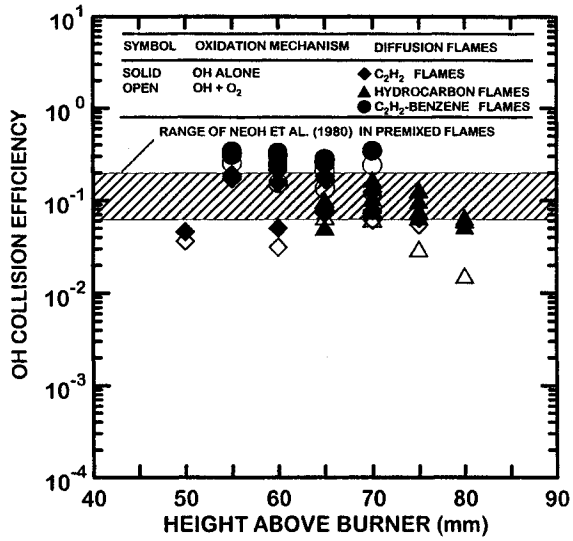

Fig. 8 Soot surface oxidation collision efficiencies assuming soot burnout due to attack by OH as a function of height above the burner. Found from the measurements of Neoh et al.[19] in premixed flames, estimated from the correlation for attack by O_2 of Nagle and Strickland-Constable[12] for the conditions of the present diffusion flames, and found from the present measurements in diffusion flames. Note that the data base for the present diffusion flames includes the measurements of Xu and Faeth[7] as well as the present investigation.